

Electronic Supplementary Material (ESI) for Journal of Materials Chemistry B
This journal is © The Royal Society of Chemistry 2020

Supporting Information

Visualizing Mitochondria and Mouse Intestine with a Fluorescent Complex of a Naphthalene-based Dipolar Dye and Serum Albumin

Jong Min An,[‡] Heejo Moon,[‡] Yejin Kim,[‡] Sangrim Kang, Youngseo Kim, Yuna Jung, Sunnam Park, Peter Verwilst,* B. Moon Kim,* Jae Seung Kang,* and Dokyoung Kim*

This PDF file includes:

1. Materials and Methods
2. Supporting Figures: S1 to S18
3. NMR (¹H, ¹³C) Spectra and HRMS of IPNHC
4. Supporting Table: S1 to S10

1. Materials and Methods

General information

The chemical reagents were purchased from Aldrich (US), TCI (Japan), Alfa Aesar (US), and Acros Organics (US). The cellular sub-organelle imaging agents, LysoTracker Deep-Red, and MitoTracker Deep-Red were purchased from ThermoFisher (US). Commercially available reagents and anhydrous solvents were used without further purification. Chemical reactions were performed under argon atmosphere. TLC (thin-layer chromatography) was performed on the pre-coated silica gel 60F-254 glass plates (Merck KGaA, Germany). ^1H and ^{13}C NMR spectra were recorded on an Agilent 400-MR DD2 Magnetic Resonance System (400 MHz) spectrophotometer in the indicated solvent. In the NMR spectra, the chemical shifts (δ) are reported in ppm, and multiplicities are indicated by s (singlet), d (doublet), t (triplet), dd (doublet of doublets), and m (multiplet). Coupling constants were reported in Hz. Chemical shifts were reported in parts per million (ppm) measured relative to the signal (0.00 ppm) of internal tetramethylsilane (TMS) in CDCl_3 (7.26 ppm for ^1H , 77.0 ppm for ^{13}C). High-resolution mass spectrometry (HRMS) of compounds was further confirmed by Ultra-High resolution ESI Q-TOF mass spectrometer (Bruker, US) at Organic Chemistry Research Center of Sogang University (Rep. of Korea). Single crystal X-ray crystallography was performed at the Center for Research Facilities in the Research Institute of Pharmaceutical Sciences of Seoul National University (Rep. of Korea), using an Agilent SuperNova X-ray diffractometer (US). All UV-vis spectrum was measured under 150 msec of shutter time, the 1.0 μm of wavelength interval, 0.5 sec of integration time, 4122 cts of min. intensity (220–350 nm), and 1277 cts of min. intensity (350–500 nm). All fluorescence spectrum was obtained under the excitation at a maximum of absorption with 1.0 μm of wavelength interval and 6000 nm/min of scan speed (irradiation time), and 150 mW lamp power. Cell imaging was conducted using a confocal laser scanning microscope (CLSM, LSM-800, Carl Zeiss, Germany). The confocal images for IPNHC in HeLa cells were obtained under 405 nm excitation (Laser power: 2.00%) with a detector (GaAsP, Detector Gain: 650 V, Detection wavelength: 400-599 nm). In the CLSM imaging, the detection wavelength was 656–700 nm (excitation wavelength: 640 nm, laser power: 0.30%). Tissue imaging was conducted using two-photon microscopy (TPM, TCS SP5, Leica microsystem, Germany).

Quantum chemical calculation

Quantum chemical calculations using density functional theory (DFT) method were performed in the Gaussian 16 package, with the B3LYP-d3 functional and 6-31+G(d) basis set, to examine the frontier orbitals and optical properties of IPNHC. The optimized structure, frontier orbitals (HOMO and LUMO), and electronic absorption and emission spectra of IPNHC in DMSO were calculated. The integral equation formalism polarizable continuum (IEFPCM) solvation model was also applied.

Fluorescence spectroscopic titration of IPNHC with BSA

IPNHC was dissolved into the BSA solution in DI H_2O (Concentration of BSA: 50 mg/mL, 1 mL). After incubation (10 min) with a vortex of the mixture, fluorescence spectra were recorded with excitation at 300 nm.

Isothermal titration calorimetry

Isothermal titration calorimetry (ITC) was performed using an affinity ITC (TA instruments, Inc, New Castle, USA) at 25 °C. Briefly, a solution of IPNHC (stock solution: 1.2 mM, solvent: phosphate buffer (pH 7.2), 10% (v/v) DMSO) was injected into the analysis vial containing BSA solution (0.2 mM) with the same solvent. In each experiment, 10 µL of the IPNHC solution was added with 5 min intervals (total 250 µL). The values are derived by integrating the peaks. The ORIGIN software (Originlab Corporation, MA, USA) was used for the calculation.

Cell culture

The immortalized human cervical cancer cell line (HeLa) was obtained from Korean Cell Line Bank (KCLB). Cells were cultured in Dulbecco's modified Eagle's media (Hyclone, US) supplemented with 10% fetal bovine serum (Hyclone) and 1% penicillin-streptomycin (Gibco). Cell lines were kept in humidified air containing 5% CO₂ at 37 °C.

Cytotoxicity analysis

The cytotoxicity of IPNHC and IPNHC-BSA complex was evaluated within the HeLa cell line by using the Cell Counting Kit-8 (CCK-8, Dojindo Molecular Tech. Inc, Japan) according to the manufacturer's protocols. The cells (5×10^3 cells per well) were seeded into 96-well plates and incubated for 24 h at 37 °C in a humidified 5% CO₂ incubator. The media was then refilled with fresh media, not containing serum or antibiotics. The cells were treated with diluted concentrations of IPNHC and IPNHC-BSA. The concentration of BSA was fixed at 50 mg/mL, and the cells were incubated for 2 h. After that, both IPNHC and IPNHC-BSA complex were removed by washing them in PBS (3 times), followed by changing the serum-free media. CCK-8 solution (10 µL, 10× working concentration) in a serum-free media was added to each well of a 96-well plate, and the cells were incubated for 2 h at 37 °C. After that, the absorbance was measured at a wavelength of 450 nm using a microplate reader (Multiskan FC, Thermo Fisher, MA, US). The percentage of cell cytotoxicity was calculated using the formula; Cell viability (%) = (Mean OD of sample × 100) / (Mean OD of the control group) (OD: optical density).

Statistical analysis

Data were presented as mean ± SDs. An unpaired two-tailed t-test was used to compare the two groups. P-values of <0.05 were considered statistically significant. Statistical tests were carried out using GraphPad InStat version 5.01 (GraphPad Software, La Jolla, CA, US).

Supporting Figures

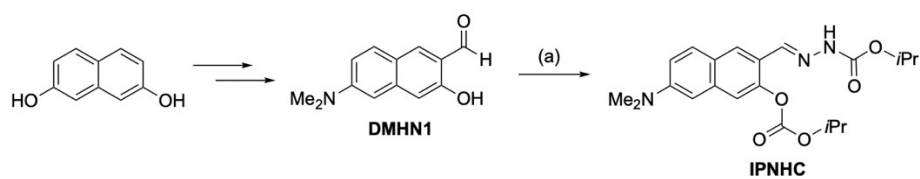


Fig. S1. Reagents and conditions: (a) diisopropyl azodicarboxylate (DIAD), triphenylphosphine (PPh₃), tetrahydrofuran (THF), 25 °C, overnight, Yield: 71%.

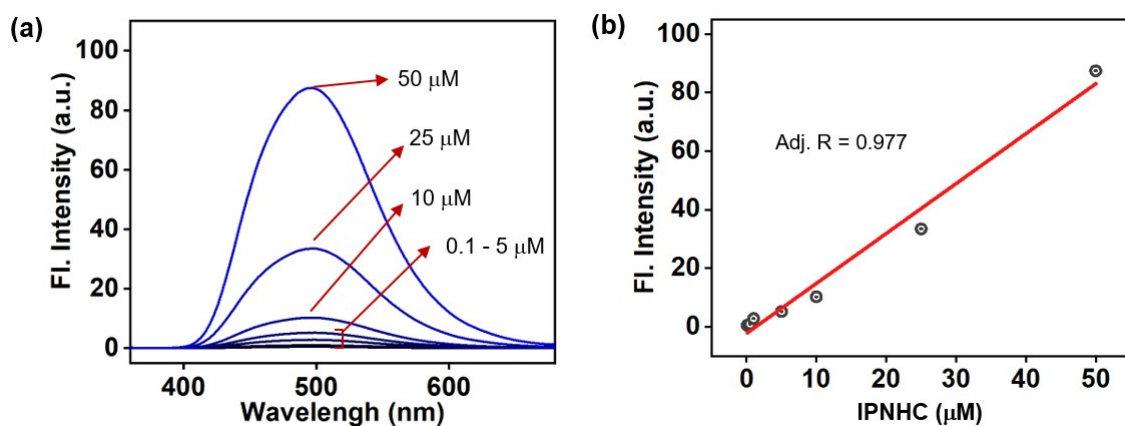


Fig. S2. (a) Emission spectra of IPNHC (0.1–50 μM) in the deionized water (DI H_2O), measured after 1 min incubation at 25 $^\circ\text{C}$. (b) Fluorescence intensity plots of IPNHC (0.1–50 μM) at 494 nm. All data were collected at room temperature, and the emission spectra were measured upon excitation at the maximum absorbance wavelength. The regression analysis was performed using OriginPro 2018.

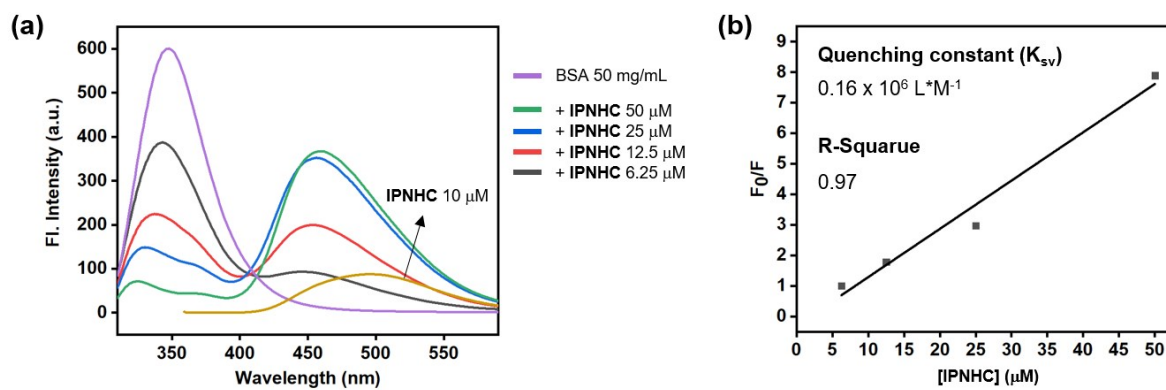


Fig. S3. (a) Emission spectra of IPNHC (6.25–50 μM) in the presence of BSA (50 mg/mL) in DI H₂O, measured after 10 min incubation at 25 °C. Excitation wavelength: 300 nm (b) Fluorescence intensity plot derived from the panel (a) at 350 nm. The linear regression analysis was performed using OriginPro 2018.

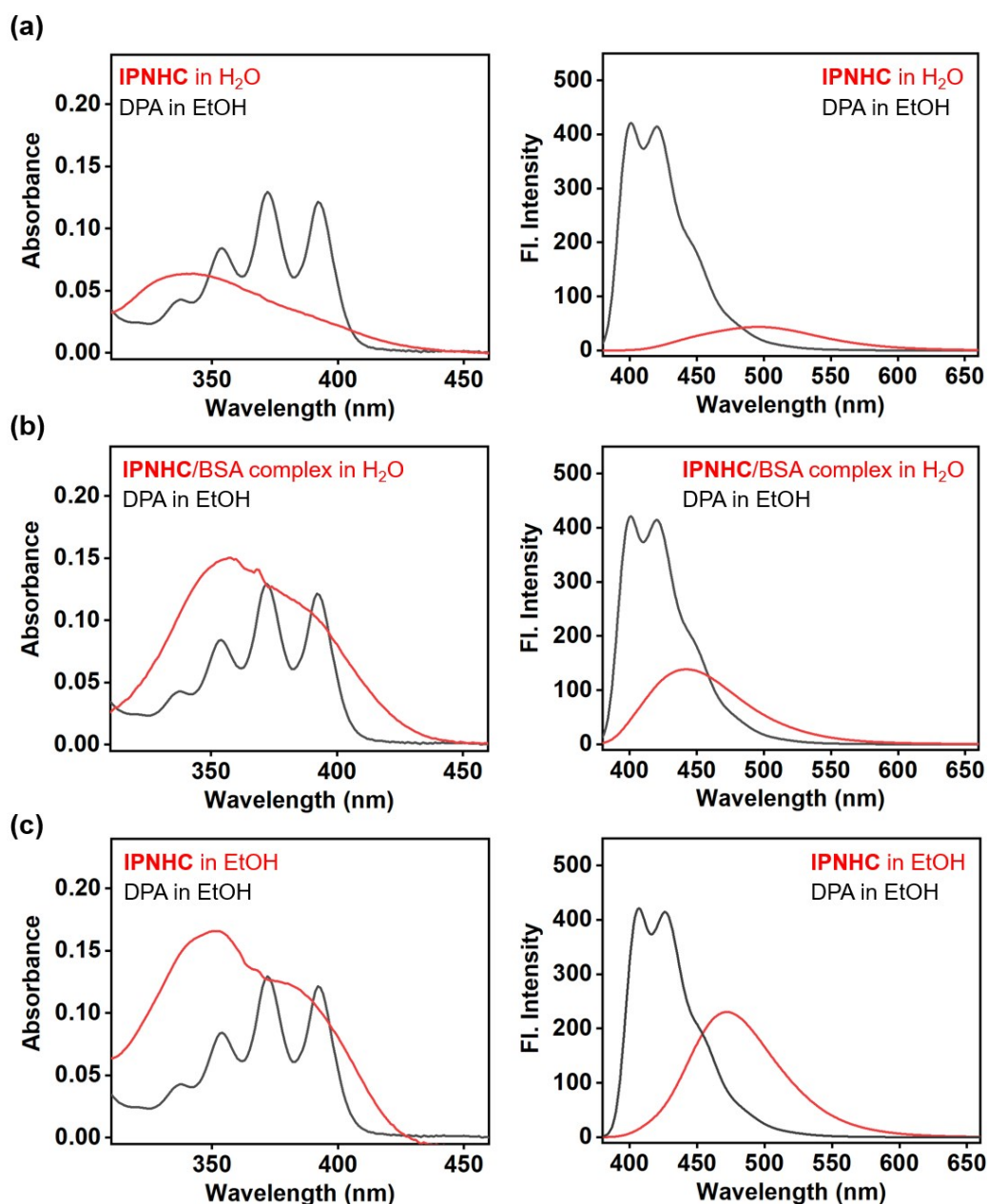


Fig. S4. (a) Absorption and emission spectra of IPNHC (10 μ M) in DI H₂O and 9,10-diphenylanthracene (DPA, 10 μ M) in EtOH. (b) Absorption and emission spectra of IPNHC-BSA complex (10 μ M of IPNHC + 50 mg/mL of BSA) in DI H₂O and DPA (10 μ M) in EtOH. (c) Absorption and emission spectra of IPNHC (10 μ M) in EtOH and DPA (10 μ M) in EtOH. All emission spectra were acquired upon excitation at the crossing point of absorption spectra. See detailed information in Table S2.

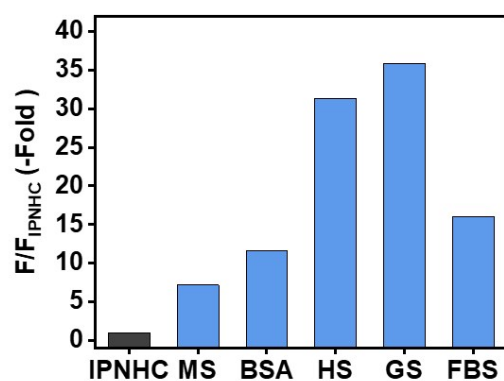


Fig. S5. Emission intensity of IPNHC (10 μ M) in the presence of mouse serum (MS, C57BL/6J mouse, a mixture of MS and PBS (1:1, v/v), total volume 1 mL), bovine serum albumin (BSA, 50 mg/mL), human serum (HS, Sigma-Aldrich product # H4522, 1 mL), goat serum (GS, Abcam product # ab7481, 1 mL), and fetal bovine serum (FBS, Hyclone product # SH30084.03, 1 mL). Emission intensity was acquired upon excitation at 360 nm at 25 °C after vortexing for 10 min, and the intensities were obtained at the maximum wavelength.

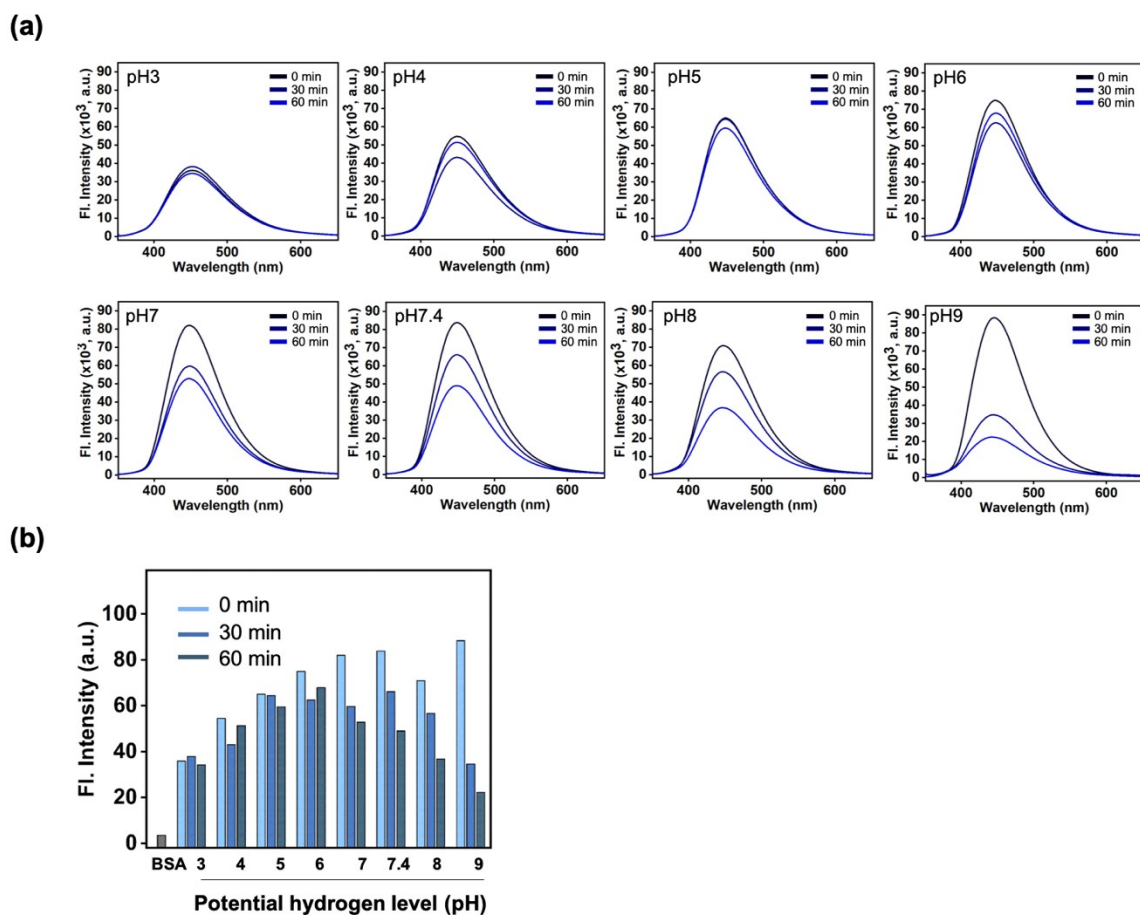


Fig. S6. Stability screening of IPNHC-BSA complex using various buffered solutions in the range of pH 3–9. (a) Emission spectra of IPNHC-BSA complex (10 μ M of IPNHC + 50 mg/mL of BSA) at various pH levels for 60 min. Emission spectra were measured upon excitation at 350 nm, for 0–60 min at 25 $^{\circ}$ C. (b) Emission intensity at the maximum wavelength from the panel (a).

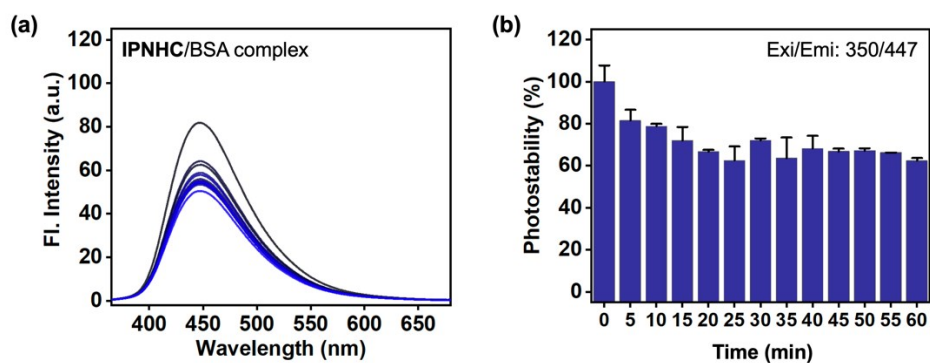


Fig. S7. Stability screening of IPNHC-BSA complex under UV light. (a) Emission spectra of IPNHC-BSA complex (10 μ M of IPNHC + 50 mg/mL of BSA in pH 5 buffer) under UV light (3 W, 365 nm) for 60 min. Emission spectra were measured upon excitation at 350 nm, for 0–60 min at 25 $^{\circ}$ C. (b) Emission intensity at the maximum wavelength from the panel (a). The error bar represents the mean \pm S.D.

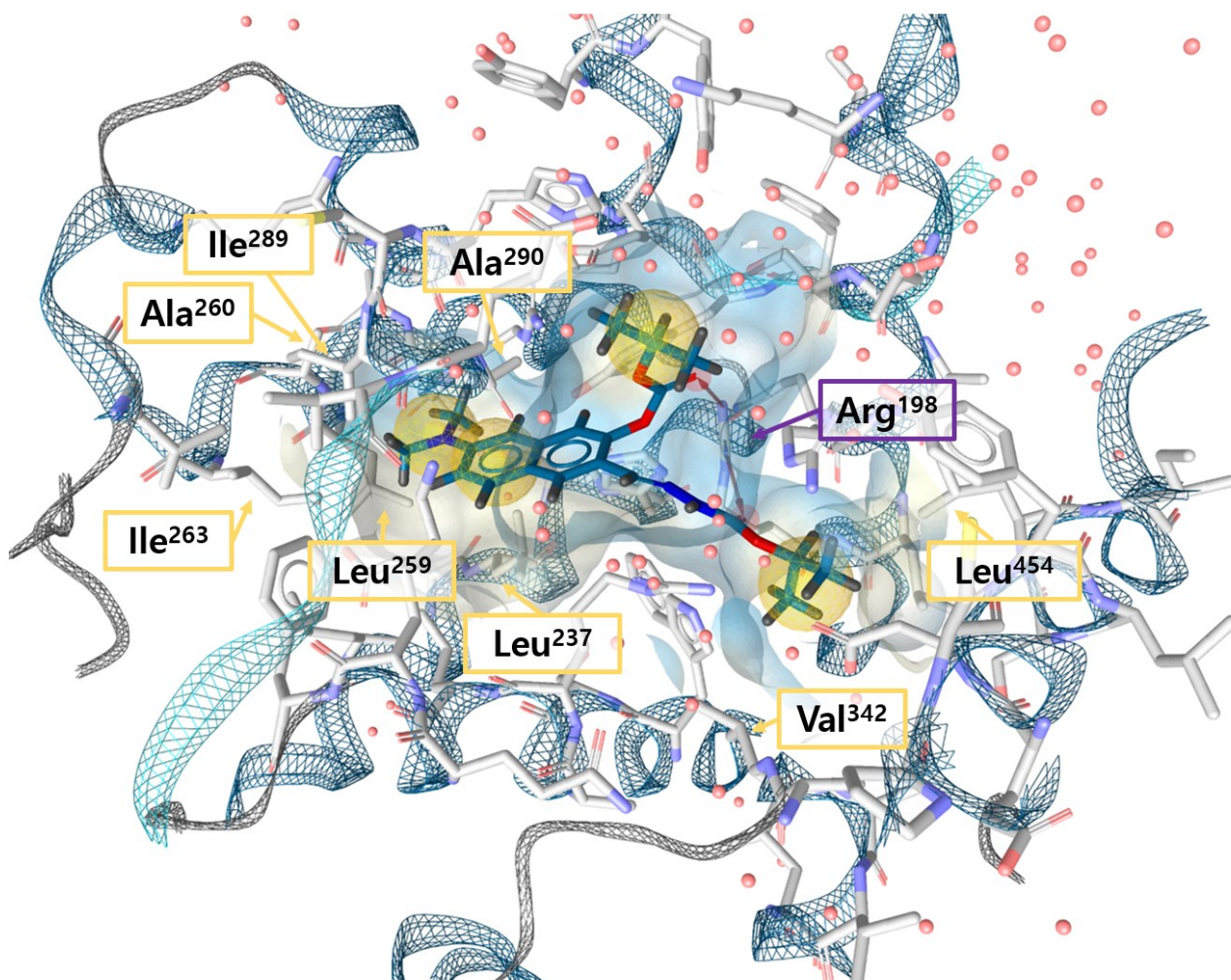


Fig. S8. Images of IPNHC (cyan) docked in the binding pocket of drug site 1 with key protein residues labeled. Yellow labels: lipophilic interaction. Purple label: Hydrogen bonding interaction.

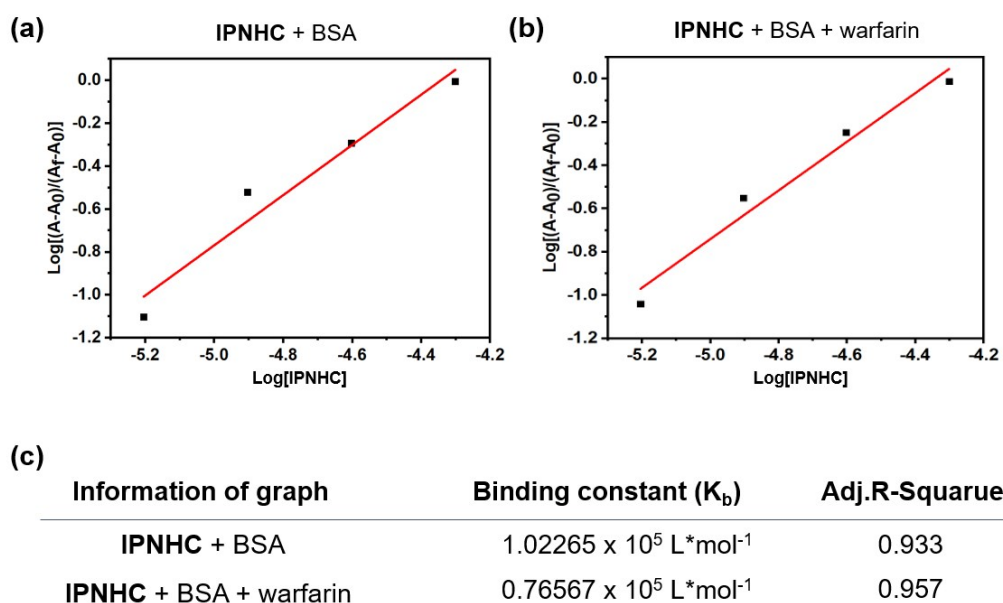


Fig. S9. Determination of binding constant (K_b) of IPNHC toward BSA. (a) Benesi-Hildebrand plots of IPNHC toward BSA. (b) Benesi-Hildebrand plots of IPNHC with BSA containing warfarin (500 μM). The concentration of BSA was fixed at 50 mg/mL in DI H_2O , and the intensity was derived from the UV/vis absorption spectra. (c) Results of binding constant via Benesi-Hildebrand calculation for IPNHC toward BSA. A_0 : absorption intensity at 360 nm absence of IPNHC, A : absorption intensity at each concentration of IPNHC (concentration 0–50 μM), and A_f : absorption intensity at 360 nm with IPNHC (concentration 50 μM , at the saturation point). $[\text{IPNHC}]$: concentration of IPNHC.

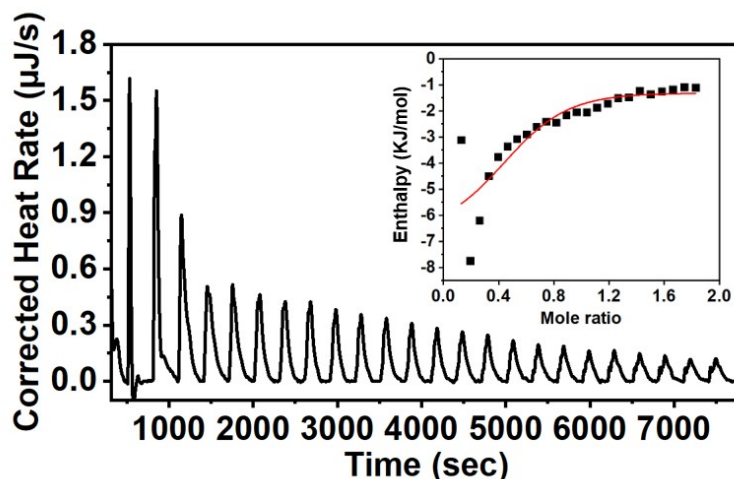


Fig. S10. Isothermal titration calorimetry (ITC) graph of IPNHC and BSA. Heat rate was recorded as a function of time during 24 successive injection of IPNHC solution at 25 °C. A solution of IPNHC (stock solution: 1.2 mM, solvent: phosphate buffer (pH 7.2), 10% (v/v) DMSO) was injected into the analysis vial containing BSA solution (0.2 mM) with the same solvent. In each experiment, 10 μL of the IPNHC solution was added with 5 min intervals (total 250 μL). Inset graph: IPNHC titration profiles toward BSA. Red line: a sigmoidal fit (used function=Boltzmann) with parameters; $n = 0.2$, K_d (M) = 2.731×10^{-6} , dH (kJ/mol) = -34.59, dS (J/mol·K) = -9.512. Parameter: stoichiometry (n), dissociation constant (K_d), enthalpy (dH), and entropy (dS).

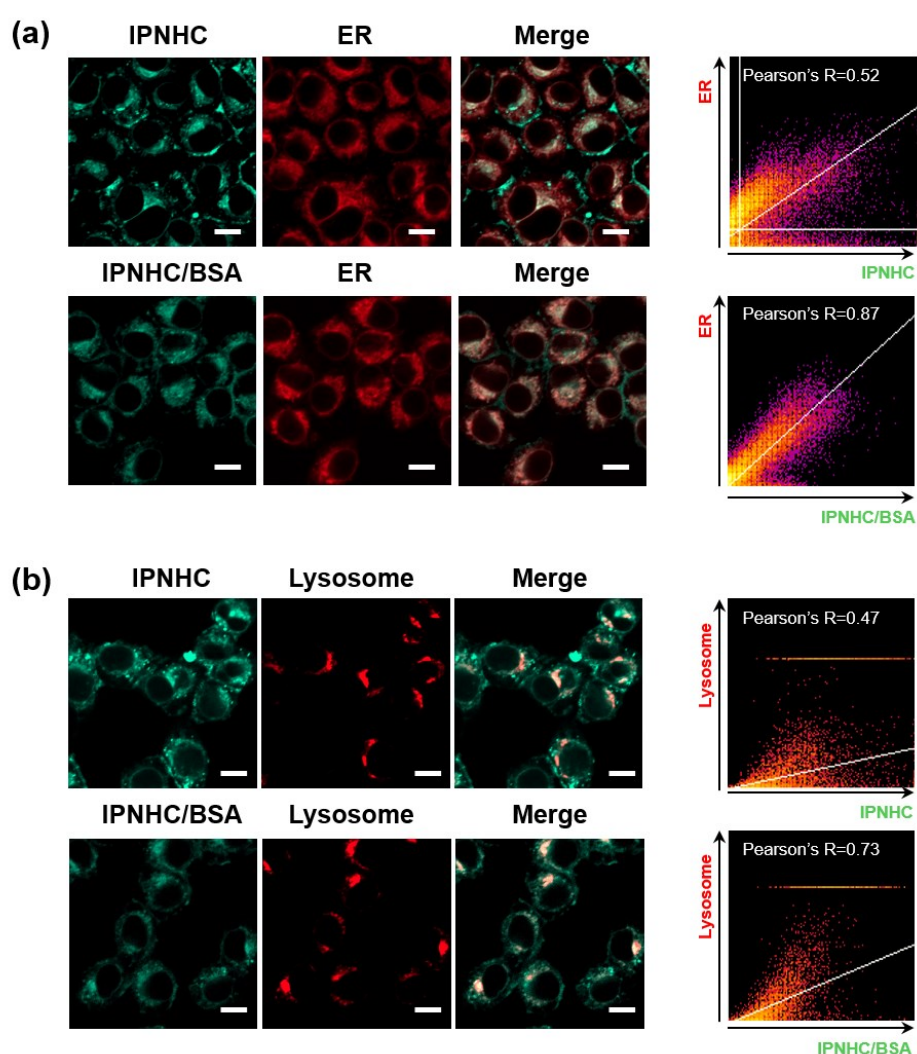


Fig. S11. CLSM images of HeLa cells with IPNHC and IPNHC-BSA complex. CLSM images of HeLa cells with treatment of IPNHC (20 μ M, Green) and IPNHC-BSA complex (20 μ M of IPNHC + 50 mg/mL of BSA), co-incubated with (a) ER-Tracker Red (indicated as ER) and (b) Lyso-Tracker Red (indicated as lysosome). Scale bar: 10 μ m. Excitation wavelength and detection channel: IPNHC and IPNHC-BSA complex (Excitation: 405 nm, Detection: 405–559 nm), tracker (ER, lysosome) (Excitation: 640 nm, Detection: 656–700 nm). Right: A linear fitting plot to obtain the Pearson correlation coefficient (PCC). The fitting data was derived from the panel (a) and (b). The PCC values were calculated using Fiji Image-J software.

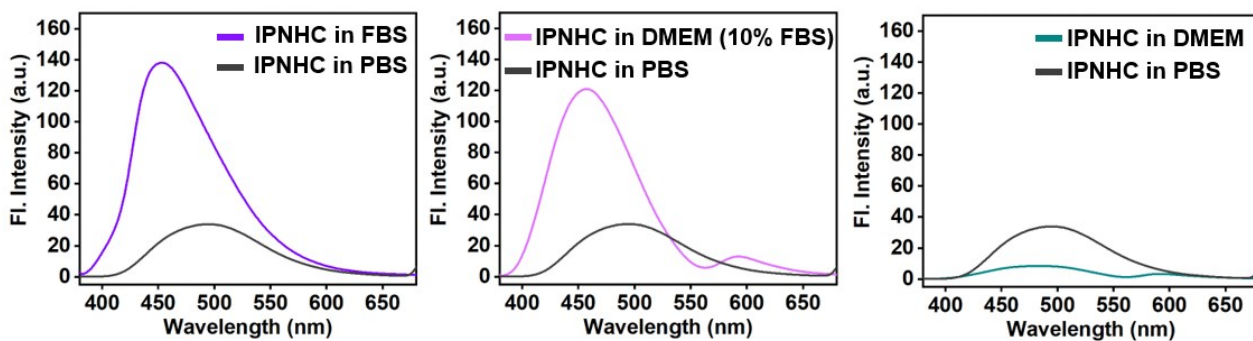


Fig. S12. Emission spectra of IPNHC (10 μ M) in PBS, FBS, DMEM, and the mixture of FBS and DMEM (10% FBS). The emission spectra were obtained under excitation at 369 nm.

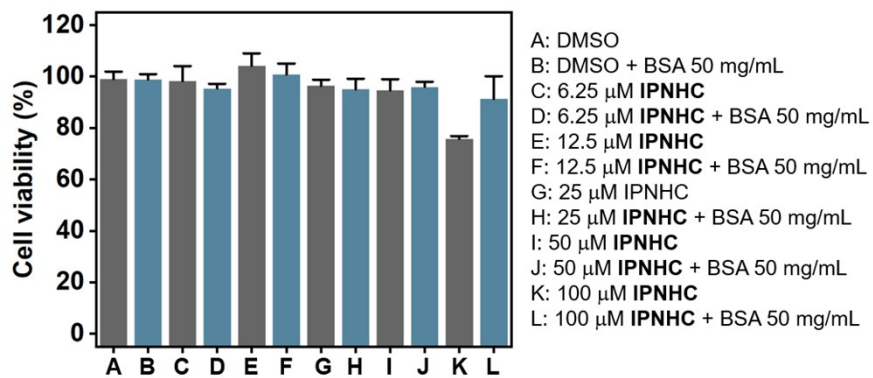


Fig. S13. Cytotoxicity assay of IPNHC and IPNHC-BSA complex in HeLa cell lines using CCK-8. The detailed conditions are described in the experiment section.

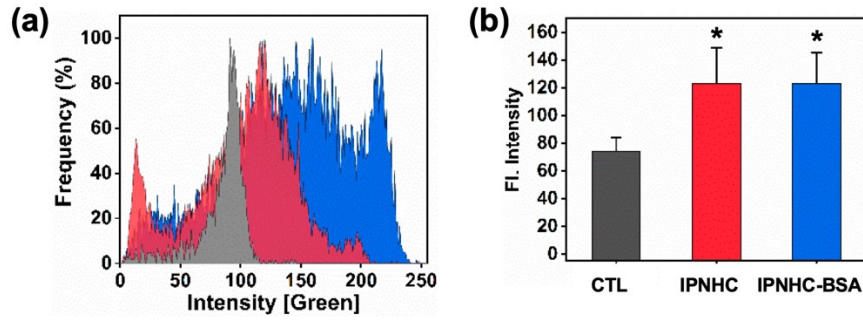


Fig. S14. (a) Fluorescence histogram profiles within the jejunum at the green channel. The signal was analyzed by Image J software. Black area: Group 1, Red area: Group 2, and Blue area: Group 3. (b) Average fluorescent intensity plot obtained from the panel (a). Each error bar represents mean \pm SD, $*p < 0.05$, and the values were calculated from the triplicate measurement. The information of each group is presented in Fig 5.

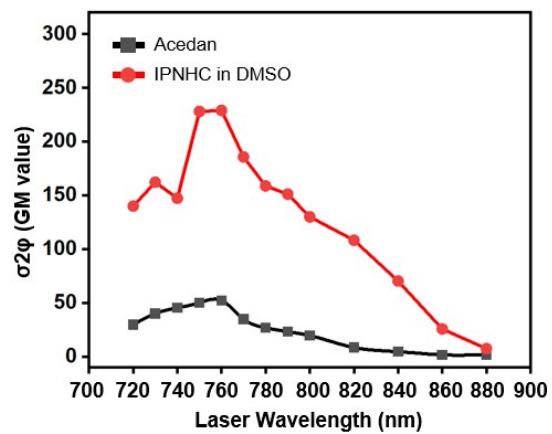


Fig. S15. Two-photon action cross-section (TPACS) value of Acedan (10 μM) and IPNHC (10 μM) in DMSO.

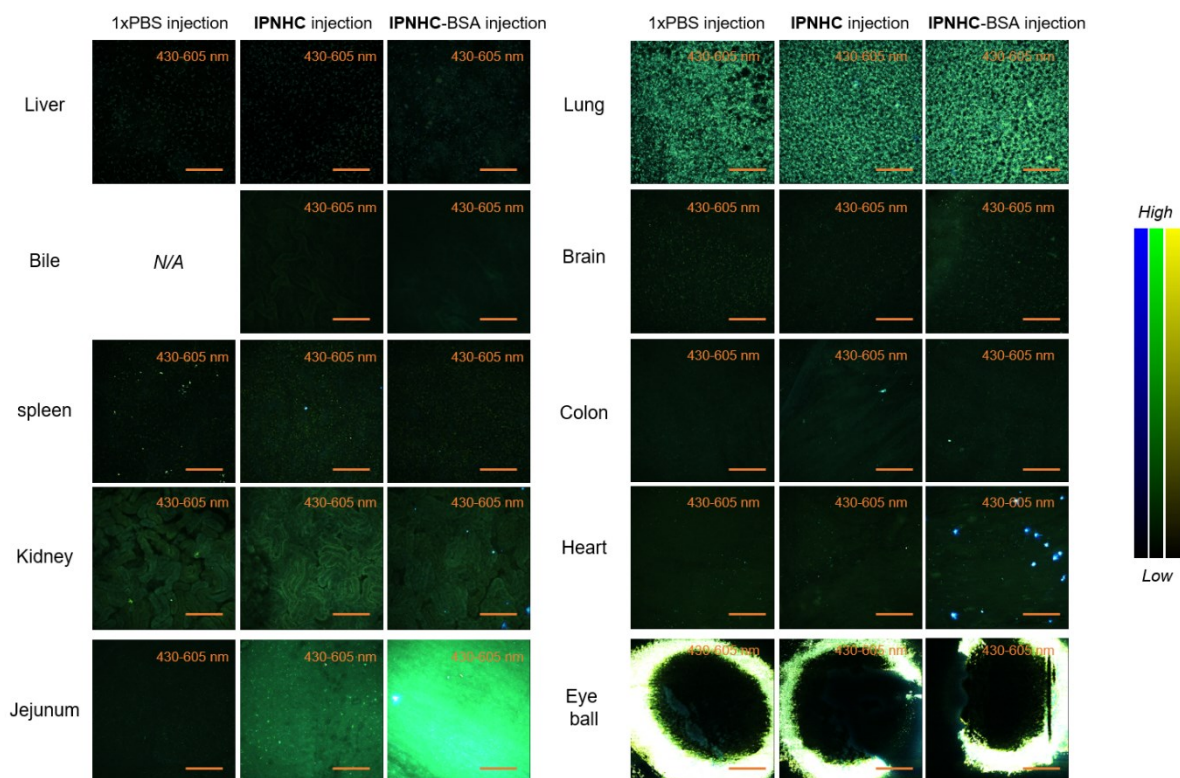


Fig. S16. TPM images of dissected mouse organs after the intravenous injection of PBS control (100 μ L), IPNHC (5.0 mg/kg in PBS, 100 μ L), and IPNHC-BSA complex (5.0 mg/kg IPNHC in 50 mg/mL of BSA in PBS, 100 μ L). TPM Excitation: 750 nm. Detection channel: 430–605 nm. Laser power: 50 mW at the focal plane. Scale bar: 200 μ m.

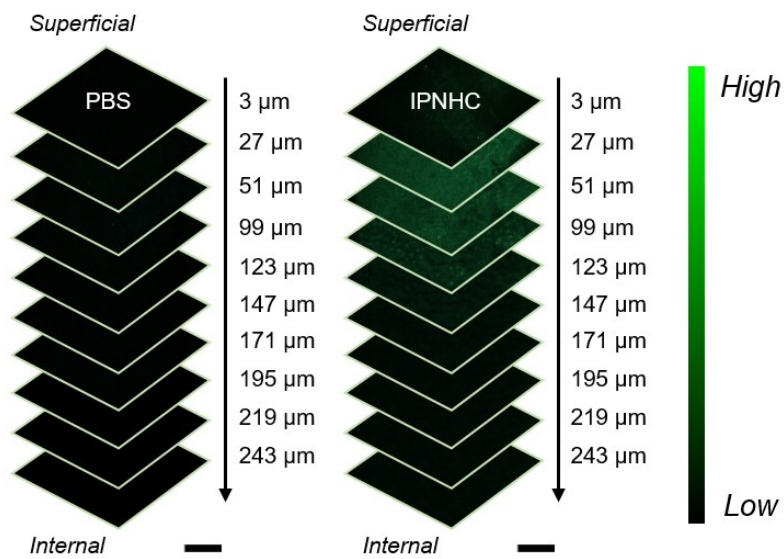


Fig. S17. Stacked TPM images of the jejunum (Group 1; PBS, Group 2; IPNHC) acquired following the indicated vertical depths (0–243 μm). Scale bar: 200 μm. The detailed conditions are described in Fig. S16 caption.

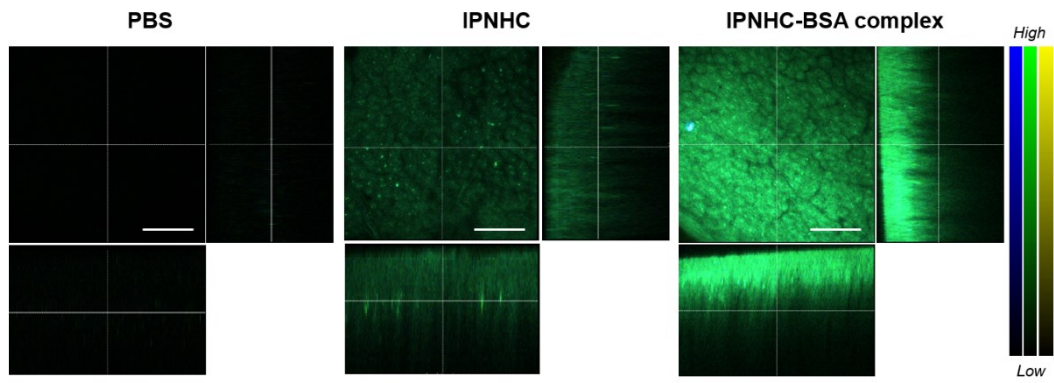
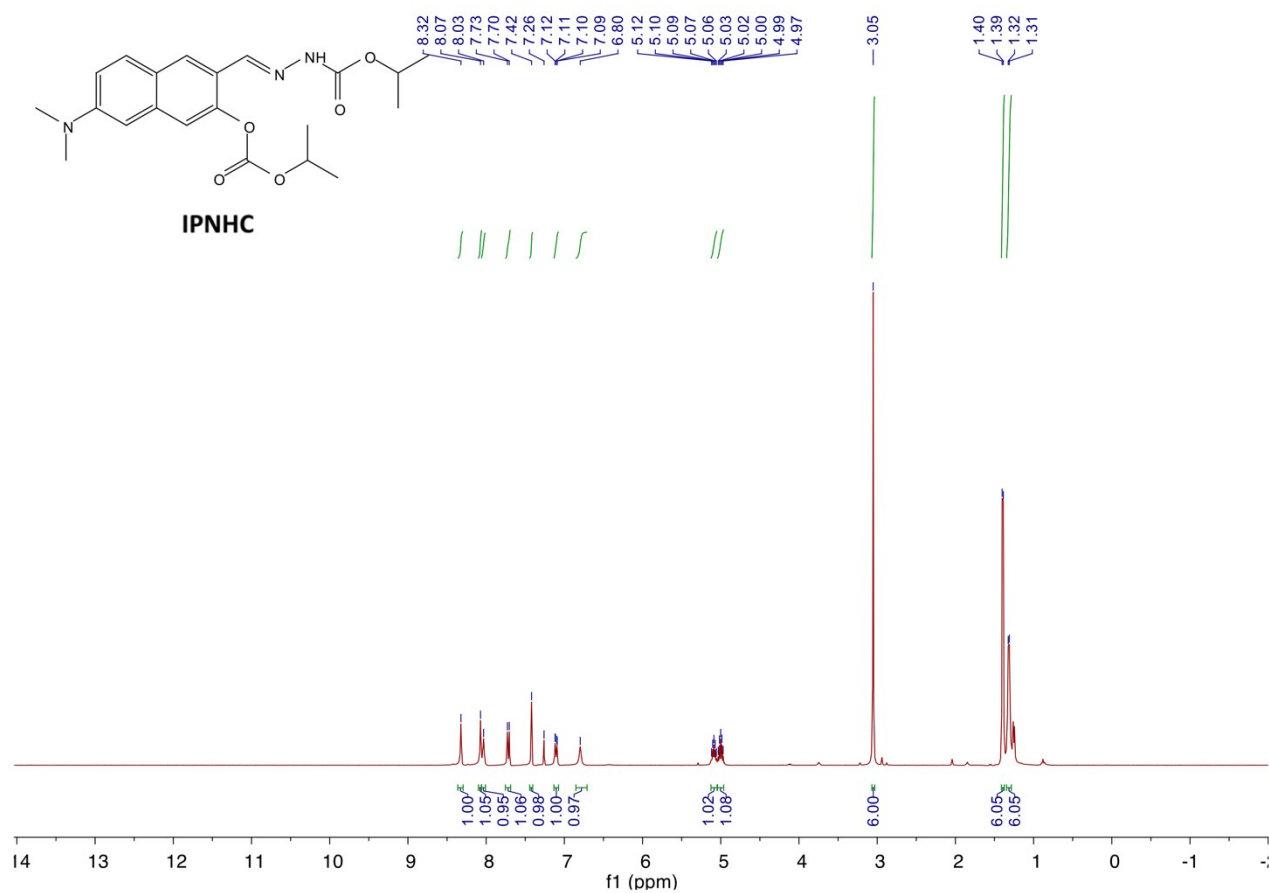
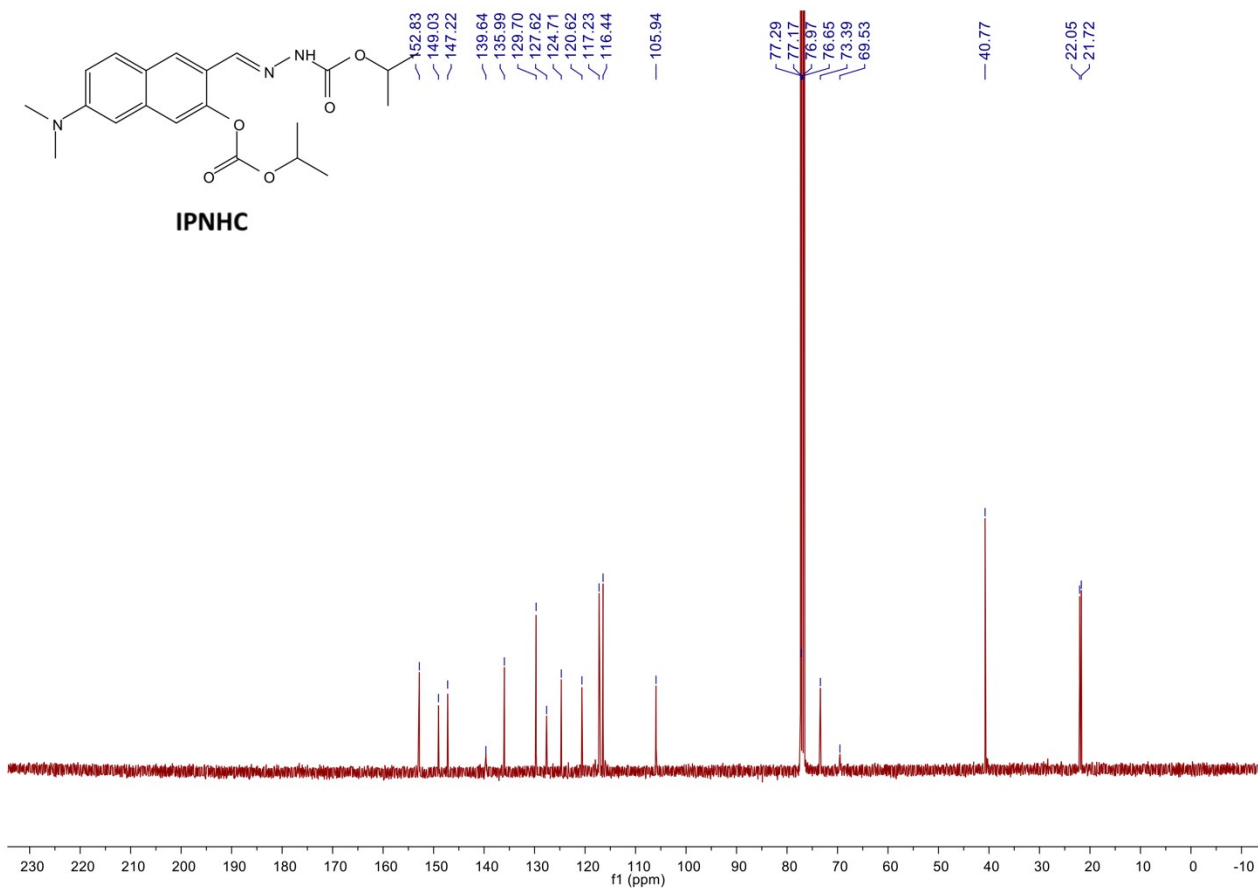


Fig. S18. TPM images (plane/lateral view) of the jejunum (Group 1; PBS, Group 2; IPNHC, Group 3; IPNHC-BSA complex). Scale bar: 200 μm . The detailed conditions are described in Fig. S16 caption.

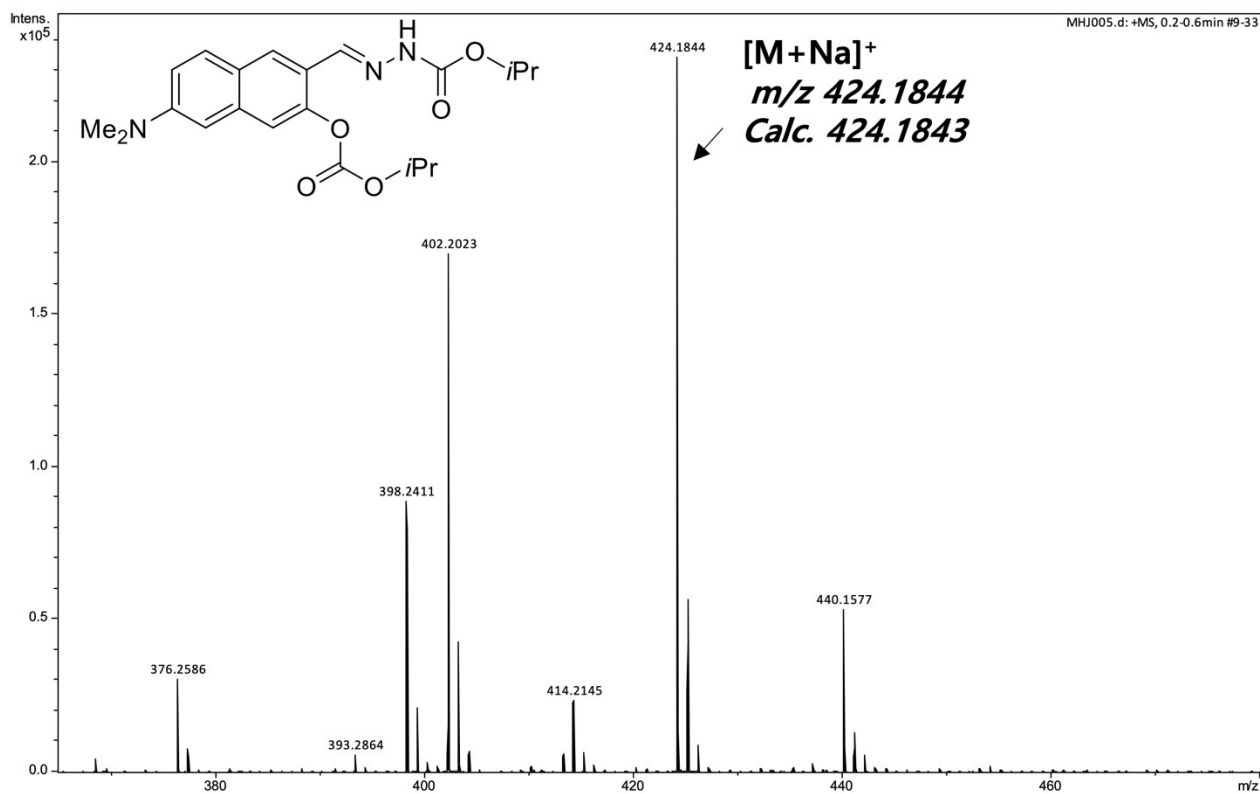
¹H NMR spectra of IPNHC



¹³C NMR spectra of IPNHC



HR-mass spectra of IPNHC



Supporting Tables

Table S1. Photophysical properties of IPNHC (10 μ M) in various solvents (EA: ethyl acetate, DMSO: dimethyl sulfoxide, IPA: *iso*-propanol, EtOH: ethanol, THF: tetrahydrofuran, DI H₂O: deionized water). ^aLog *P* values were calculated using ACDLog *P* database.

| Compounds | Solvents | λ_{abs} (nm) | ϵ (L mol ⁻¹ cm ⁻¹) | λ_{fl} (nm) | Stokes shift | ^a Log <i>P</i> |
|--------------|------------------------------------|-----------------------------|--|----------------------------|--------------|---------------------------|
| IPNHC | EA | 345 | 167,720 | 443 | 98 | 3.99 |
| | DMSO | 352 | 154,160 | 468 | 116 | |
| | IPA | 345 | 187,440 | 456 | 111 | |
| | EtOH | 345 | 128,400 | 470 | 125 | |
| | THF | 347 | 164,700 | 444 | 97 | |
| | DI H ₂ O | 340 | 36,820 | 495 | 155 | |
| | ACN | 311 | 133,270 | 444 | 133 | |
| | 20% EtOH in DI H ₂ O | 346 | 128,520 | 492 | 146 | |
| DMHN1 | - | - | - | - | - | 2.95 |

Table S2. Experimental parameters for determining the quantum yield of IPNHC and IPNHC-BSA complex. DPA: 9,10-diphenylanthracene. QY: quantum yield. EtOH: ethanol. DI H₂O: deionized water.

| | DPA | IPNHC | DPA | IPNHC | IPNHC-BSA complex |
|---------------------------------|---------------------|--------------------------------|---------------------|---------------------|--------------------------------|
| $\lambda_{\text{Exi max}}$ (nm) | 349 | 349 | 371 | 371 | 371 |
| QY _{ref} | 0.88 | - | 0.88 | - | - |
| η | 1.356 (EtOH) | 1.333 (DI H ₂ O) | 1.356 (EtOH) | 1.356 (EtOH) | 1.333 (DI H ₂ O) |
| I | 24619×10^3 | 4919×10^3 | 24619×10^3 | 19653×10^3 | 12511×10^3 |
| QY | - | 0.1875 | - | 0.7166 | 0.4677 |

Crystallographic Data

Crystallographic data of IPNHC

The crystal structure was deposited at the Cambridge Crystallographic Data Center (CCDC).

CCDC: Deposition Number 1997498

Table S3. Crystal Data and Structure Refinement for IPNHC

| | |
|---|--|
| Empirical formula | C ₂₁ H ₂₇ N ₃ O ₅ |
| Formula weight | 401.45 |
| Temperature | 294.34(11) K |
| Wavelength | Mo K α (λ = 0.71073 Å) |
| Crystal system | Monoclinic |
| Space group | P2 ₁ /c |
| <i>a</i> | 22.1636(12) Å |
| <i>b</i> | 12.4096(7) Å |
| <i>c</i> | 8.0919(7) Å |
| Volume | 2200.8(3) Å ³ |
| Z, Calculated density | 4, 1.212 g/cm ³ |
| Absorption coefficient | 0.087 mm ⁻¹ |
| <i>F</i> (000) | 856.0 |
| Limiting indices | -27 ≤ <i>h</i> ≤ 22, -15 ≤ <i>k</i> ≤ 15, -10 ≤ <i>l</i> ≤ 10 |
| Reflections collected / unique | 23731 / 4552 [<i>R</i> _{int} = 0.0729, <i>R</i> _{sigma} = 0.0511] |
| Data / restraints / parameters | 4552 / 24 / 289 |
| Goodness-of-fit on <i>F</i> ² | 1.047 |
| Final R indices [<i>I</i> > 2σ _{<i>i</i>}] | <i>R</i> ₁ = 0.0689, <i>wR</i> ₂ = 0.1562 |
| Final R indices (all data) | <i>R</i> ₁ = 0.1120, <i>wR</i> ₂ = 0.1835 |
| Largest diff. peak and hole | 0.24 and -0.22 e. Å ⁻³ |

Table S4. Fractional Atomic Coordinates ($\times 10^4$) and Equivalent Isotropic Displacement Parameters ($\text{\AA}^2 \times 10^3$) for IPNHC. U_{eq} is defined as 1/3 of the trace of the U_{ij} tensor.

| Atom | x | y | z | U (eq) |
|------|-------------|------------|----------|-----------|
| O2 | 7522.9(8) | 4615.6(14) | 2262(3) | 58.2(5) |
| C8 | 6578.4(11) | 6607(2) | -1417(3) | 43.8(6) |
| C6 | 7488.2(11) | 6239(2) | 592(3) | 45.0(6) |
| N2 | 8401.8(9) | 7273.8(18) | 884(3) | 52.3(6) |
| C5 | 8085.5(11) | 6564(2) | 1479(4) | 48.0(6) |
| O5 | 9241.7(9) | 8673.4(16) | -53(3) | 62.1(6) |
| C7 | 7167.5(11) | 6872(2) | -629(3) | 46.6(6) |
| C15 | 6304.8(11) | 5635(2) | -980(3) | 45.1(6) |
| C17 | 7198.6(11) | 5288(2) | 1015(3) | 46.6(6) |
| O3 | 7045.3(10) | 5446.4(19) | 4171(3) | 78.2(7) |
| C9 | 6230.2(12) | 7290(2) | -2579(4) | 53.7(7) |
| C14 | 5698.2(12) | 5395(2) | -1699(4) | 55.4(7) |
| C4 | 9320.4(12) | 8245(2) | 1304(4) | 53.0(7) |
| C16 | 6642.7(12) | 4974(2) | 250(4) | 50.5(7) |
| C13 | 5361.8(12) | 6088(3) | -2808(4) | 58.9(8) |
| N3 | 8942.9(9) | 7536(2) | 1875(3) | 59.5(7) |
| O4 | 9803.6(9) | 8410.3(18) | 2490(3) | 75.2(7) |
| C18 | 7391.6(12) | 4788(2) | 3818(4) | 50.3(7) |
| O1 | 7714.0(11) | 4116.4(18) | 4827(3) | 79.9(7) |
| C10 | 5648.7(12) | 7050(3) | -3242(4) | 61.7(8) |
| N1 | 4767.4(12) | 5857(3) | -3494(4) | 84.5(9) |
| C3 | 10292.3(15) | 9074(3) | 2028(5) | 78.7(10) |
| C12 | 4495.4(15) | 4846(3) | -3114(5) | 94.0(13) |
| C19 | 7666.6(17) | 4214(3) | 6625(4) | 75.8(9) |
| C11 | 4372.6(16) | 6667(4) | -4344(6) | 115.2(16) |
| C1 | 10645(2) | 9467(5) | 3611(6) | 155(2) |
| C2 | 10667(2) | 8433(5) | 1029(8) | 156(2) |
| C020 | 7563(8) | 3117(6) | 7238(9) | 158(5) |
| C20' | 7230(20) | 3440(40) | 6910(70) | 86(14) |
| C021 | 8214(3) | 4768(10) | 7413(9) | 128(4) |
| C21' | 8310(20) | 3970(70) | 7570(60) | 118(19) |

Table S5. Anisotropic Displacement Parameters ($\text{\AA}^2 \times 10^3$) for IPNHC. The Anisotropic displacement factor exponent takes the form: $-2\pi^2[h^2a^*2U_{11}+2hka^*b^*U_{12}+\dots]$.

| Atom | U_{11} | U_{22} | U_{33} | U_{23} | U_{13} | U_{12} |
|------|----------|----------|----------|-----------|-----------|-----------|
| O2 | 62.5(12) | 51.5(11) | 60.2(13) | 7.7(9) | 7.4(10) | 15.9(9) |
| C8 | 38.4(13) | 48.1(14) | 44.9(15) | -0.5(12) | 6.1(11) | -3.6(11) |
| C6 | 37.8(13) | 47.5(14) | 49.5(17) | -1.7(12) | 5.6(11) | 1.2(11) |
| N2 | 40.4(12) | 63.2(14) | 50.3(15) | 2.7(11) | -3.4(10) | -7.0(10) |
| C5 | 36.4(13) | 55.2(15) | 50.3(17) | 2.5(13) | -0.6(12) | 5.6(12) |
| O5 | 60.3(12) | 72.5(13) | 49.3(13) | 8.1(10) | -5.9(10) | -12.7(10) |
| C7 | 41.7(14) | 46.2(14) | 52.1(17) | 3.1(12) | 7.6(12) | -6.6(11) |
| C15 | 39.1(13) | 50.6(15) | 45.5(16) | -3.9(12) | 6.1(11) | -5.6(11) |
| C17 | 46.3(15) | 45.3(14) | 48.2(17) | 2.4(12) | 6.8(12) | 6.6(11) |
| O3 | 76.6(14) | 90.9(16) | 65.6(16) | 2.6(12) | 5.6(12) | 34.3(13) |
| C9 | 49.1(15) | 56.3(16) | 53.7(18) | 8.2(13) | 1.1(13) | -7.1(12) |
| C14 | 49.4(16) | 60.6(17) | 55.8(19) | -2.8(14) | 6.5(14) | -15.8(13) |
| C4 | 41.3(15) | 62.7(17) | 51.8(19) | -2.3(15) | -3.5(13) | -6.1(12) |
| C16 | 50.2(15) | 42.3(14) | 59.9(19) | 0.2(13) | 11.1(14) | -8.9(12) |
| C13 | 44.4(16) | 75(2) | 55.4(19) | -11.4(15) | 2.3(14) | -10.6(14) |
| N3 | 45.7(13) | 79.4(16) | 48.2(15) | 11.5(12) | -10.2(11) | -13.4(12) |
| O4 | 58.0(12) | 99.8(16) | 60.3(14) | 17.1(12) | -15.8(10) | -33.3(11) |
| C18 | 46.3(15) | 44.2(15) | 58.2(19) | 3.5(13) | 0.7(13) | -1.4(12) |
| O1 | 99.9(17) | 74.5(14) | 62.2(15) | 16.2(12) | 2.6(12) | 35.2(13) |
| C10 | 47.4(16) | 75(2) | 58(2) | 5.5(15) | -6.1(14) | 0.7(14) |
| N1 | 48.1(15) | 105(2) | 94(2) | -6.0(19) | -9.8(15) | -15.7(15) |
| C3 | 58.6(19) | 93(2) | 79(3) | 18(2) | -7.4(18) | -31.2(18) |
| C12 | 59(2) | 137(3) | 85(3) | -17(2) | 8.5(19) | -40(2) |
| C19 | 86(2) | 77(2) | 62(2) | 11.5(17) | 2.4(17) | 14.1(18) |
| C11 | 55(2) | 149(4) | 130(4) | 2(3) | -23(2) | 7(2) |
| C1 | 140(4) | 191(5) | 118(4) | 9(4) | -29(3) | -102(4) |
| C2 | 77(3) | 175(5) | 225(7) | -9(5) | 49(4) | -12(3) |
| C020 | 282(14) | 96(5) | 99(5) | 31(4) | 38(6) | -17(6) |
| C20' | 93(16) | 86(17) | 81(17) | 1(9) | 17(9) | 1(9) |
| C021 | 114(5) | 164(9) | 105(5) | -54(5) | 15(3) | -28(5) |
| C21' | 120(20) | 120(20) | 110(20) | 2(10) | 5(10) | 3(10) |

Table S6. Bond Lengths for IPNHC

| Atom | Atom | Length/Å | Atom | Atom | Length/Å |
|------|------|----------|------|------|----------|
| O2 | C17 | 1.419(3) | C14 | C13 | 1.379(4) |
| O2 | C18 | 1.351(3) | C4 | N3 | 1.343(3) |
| C8 | C7 | 1.404(3) | C4 | O4 | 1.343(3) |
| C8 | C15 | 1.418(3) | C13 | C10 | 1.420(4) |
| C8 | C9 | 1.408(4) | C13 | N1 | 1.381(4) |
| C6 | C5 | 1.465(3) | O4 | C3 | 1.453(4) |
| C6 | C7 | 1.374(4) | C18 | O1 | 1.303(3) |
| C6 | C17 | 1.410(3) | O1 | C19 | 1.479(4) |
| N2 | C5 | 1.265(3) | N1 | C12 | 1.445(5) |
| N2 | N3 | 1.379(3) | N1 | C11 | 1.439(5) |
| O5 | C4 | 1.209(3) | C3 | C1 | 1.480(5) |
| C15 | C14 | 1.415(3) | C3 | C2 | 1.475(6) |
| C15 | C16 | 1.414(4) | C19 | C020 | 1.478(7) |
| C17 | C16 | 1.351(4) | C19 | C20' | 1.40(5) |
| O3 | C18 | 1.185(3) | C19 | C021 | 1.457(6) |
| C9 | C10 | 1.353(4) | C19 | C21' | 1.55(5) |

Table S7. Bond Angles for IPNHC

| Atom | Atom | Atom | Angle/° | Atom | Atom | Atom | Angle/° |
|------|------|------|----------|------|------|------|----------|
| C18 | O2 | C17 | 114.4(2) | C14 | C13 | C10 | 117.8(2) |
| C7 | C8 | C15 | 119.3(2) | C14 | C13 | N1 | 121.5(3) |
| C7 | C8 | C9 | 122.8(2) | N1 | C13 | C10 | 120.7(3) |
| C9 | C8 | C15 | 117.8(2) | C4 | N3 | N2 | 119.2(2) |
| C7 | C6 | C5 | 121.9(2) | C4 | O4 | C3 | 116.6(2) |
| C7 | C6 | C17 | 116.6(2) | O3 | C18 | O2 | 124.8(3) |
| C17 | C6 | C5 | 121.4(2) | O3 | C18 | O1 | 127.2(3) |
| C5 | N2 | N3 | 115.2(2) | O1 | C18 | O2 | 108.0(2) |
| N2 | C5 | C6 | 121.1(2) | C18 | O1 | C19 | 116.8(2) |
| C6 | C7 | C8 | 122.6(2) | C9 | C10 | C13 | 121.5(3) |
| C14 | C15 | C8 | 119.5(2) | C13 | N1 | C12 | 119.9(3) |
| C16 | C15 | C8 | 117.8(2) | C13 | N1 | C11 | 121.5(3) |
| C16 | C15 | C14 | 122.6(2) | C11 | N1 | C12 | 117.7(3) |
| C6 | C17 | O2 | 117.7(2) | O4 | C3 | C1 | 106.4(3) |
| C16 | C17 | O2 | 119.1(2) | O4 | C3 | C2 | 109.7(3) |
| C16 | C17 | C6 | 123.1(2) | C2 | C3 | C1 | 112.6(4) |
| C10 | C9 | C8 | 121.8(3) | O1 | C19 | C21' | 106(2) |
| C13 | C14 | C15 | 121.6(3) | C020 | C19 | O1 | 107.0(4) |
| O5 | C4 | N3 | 126.0(2) | C20' | C19 | O1 | 105(2) |
| O5 | C4 | O4 | 125.0(3) | C20' | C19 | C21' | 113(2) |
| N3 | C4 | O4 | 109.0(3) | C021 | C19 | O1 | 107.0(4) |
| C17 | C16 | C15 | 120.5(2) | C021 | C19 | C020 | 116.7(5) |

Table S8. Torsion Angles for IPNHC

| A | B | C | D | Angle/° | A | B | C | D | Angle/° |
|-----|-----|-----|-----|----------|-----|-----|-----|------|-----------|
| O2 | C17 | C16 | C15 | 179.1(2) | C17 | C6 | C7 | C8 | 0.7(4) |
| O2 | C18 | O1 | C19 | 176.4(2) | O3 | C18 | O1 | C19 | -3.0(4) |
| C8 | C15 | C14 | C13 | -0.6(4) | C9 | C8 | C7 | C6 | 175.2(3) |
| C8 | C15 | C16 | C17 | 2.3(4) | C9 | C8 | C15 | C14 | -0.8(4) |
| C8 | C9 | C10 | C13 | -0.6(5) | C9 | C8 | C15 | C16 | -176.9(2) |
| C6 | C17 | C16 | C15 | -3.5(4) | C14 | C15 | C16 | C17 | -173.7(3) |
| C5 | C6 | C7 | C8 | 175.9(2) | C14 | C13 | C10 | C9 | -0.8(5) |
| C5 | C6 | C17 | O2 | -4.0(4) | C14 | C13 | N1 | C12 | -3.0(5) |
| C5 | C6 | C17 | C16 | 178.6(2) | C14 | C13 | N1 | C11 | 166.0(4) |
| C5 | N2 | N3 | C4 | 176.9(3) | C4 | O4 | C3 | C1 | 159.7(4) |
| O5 | C4 | N3 | N2 | -2.1(5) | C4 | O4 | C3 | C2 | -78.2(4) |
| O5 | C4 | O4 | C3 | -6.4(5) | C16 | C15 | C14 | C13 | 175.3(3) |
| C7 | C8 | C15 | C14 | 176.4(2) | N3 | N2 | C5 | C6 | 177.5(2) |
| C7 | C8 | C15 | C16 | 0.2(4) | N3 | C4 | O4 | C3 | 174.0(3) |
| C7 | C8 | C9 | C10 | 175.6(3) | O4 | C4 | N3 | N2 | 177.6(2) |
| C7 | C6 | C5 | N2 | -19.0(4) | C18 | O2 | C17 | C6 | 95.1(3) |
| C7 | C6 | C17 | O2 | 179.4(2) | C18 | O2 | C17 | C16 | -87.4(3) |
| C7 | C6 | C17 | C16 | 2.0(4) | C18 | O1 | C19 | C020 | 131.8(7) |
| C15 | C8 | C7 | C6 | -1.8(4) | C18 | O1 | C19 | C20' | 97(2) |
| C15 | C8 | C9 | C10 | 1.4(4) | C18 | O1 | C19 | C021 | -102.4(6) |
| C15 | C14 | C13 | C10 | 1.4(4) | C18 | O1 | C19 | C21' | -144(3) |
| C15 | C14 | C13 | N1 | 179.3(3) | C10 | C13 | N1 | C12 | 176.3(3) |
| C17 | O2 | C18 | O3 | -1.1(4) | C10 | C13 | N1 | C11 | -14.7(5) |
| C17 | O2 | C18 | O1 | 179.5(2) | N1 | C13 | C10 | C9 | 179.9(3) |
| C17 | C6 | C5 | N2 | 164.6(3) | | | | | |

Table S9. Hydrogen Atom Coordinates ($\text{\AA}\times 10^4$) and Isotropic Displacement Parameters ($\text{\AA}^2\times 10^3$) for IPNHC

| Atom | <i>x</i> | <i>y</i> | <i>z</i> | U (eq) |
|------|----------|----------|----------|--------|
| H5 | 8234.47 | 6242.47 | 2496.53 | 58 |
| H7 | 7347.75 | 7500.81 | -946.36 | 56 |
| H9 | 6404.6 | 7923.22 | -2899.5 | 64 |
| H14 | 5521.83 | 4753.34 | -1416.87 | 66 |
| H16 | 6481.25 | 4319.82 | 533.47 | 61 |
| H3 | 9037.31 | 7249.02 | 2846.19 | 71 |
| H10 | 5432.18 | 7524.99 | -3997.69 | 74 |
| H3A | 10116.56 | 9690.06 | 1366.43 | 94 |
| H12A | 4741.71 | 4260.43 | -3409.83 | 141 |
| H12B | 4093.07 | 4791.26 | -3739.61 | 141 |
| H12C | 4470.83 | 4813.55 | -1940.67 | 141 |
| H19 | 7310.98 | 4660.32 | 6744.59 | 91 |
| H19A | 7534.48 | 4938.92 | 6890.82 | 91 |
| H11A | 4283.23 | 7198.84 | -3553.86 | 173 |
| H11B | 3999.85 | 6337.22 | -4860.37 | 173 |
| H11C | 4571.32 | 7004.5 | -5184.33 | 173 |
| H1A | 10407.59 | 9989.26 | 4107.61 | 232 |
| H1B | 11016.92 | 9793.2 | 3387.07 | 232 |
| H1C | 10738.62 | 8872.22 | 4364.48 | 232 |
| H2A | 10828.89 | 7816.61 | 1662.5 | 235 |
| H2B | 10996.45 | 8867 | 754.93 | 235 |
| H2C | 10418.81 | 8197.12 | 18.96 | 235 |
| H02A | 7596.52 | 3127.47 | 8434.18 | 238 |
| H02B | 7862.54 | 2634.53 | 6910.97 | 238 |
| H02C | 7162.43 | 2876.69 | 6766.04 | 238 |
| H20A | 6842.4 | 3630.83 | 6305.57 | 129 |
| H20B | 7207.81 | 3408.76 | 8084.96 | 129 |
| H20C | 7353.35 | 2746.95 | 6541.92 | 129 |
| H02D | 8224.03 | 5482.53 | 6961.34 | 192 |
| H02E | 8568.75 | 4377.5 | 7200.84 | 192 |
| H02F | 8211.52 | 4810.64 | 8596.48 | 192 |
| H21A | 8411.43 | 3227.49 | 7383.68 | 177 |
| H21B | 8316.18 | 4086.17 | 8742.16 | 177 |
| H21C | 8602.97 | 4429.04 | 7164.06 | 177 |

Table S10. Atomic Occupancy for IPNHC

| Atom | Occupancy | Atom | Occupancy | Atom | Occupancy |
|-------------|------------------|-------------|------------------|-------------|------------------|
| H19 | 0.885(19) | H19A | 0.115(19) | C020 | 0.885(19) |
| H02A | 0.885(19) | H02B | 0.885(19) | H02C | 0.885(19) |
| C20' | 0.115(19) | H20A | 0.115(19) | H20B | 0.115(19) |
| H20C | 0.115(19) | C021 | 0.885(19) | H02D | 0.885(19) |
| H02E | 0.885(19) | H02F | 0.885(19) | C21' | 0.115(19) |
| H21A | 0.115(19) | H21B | 0.115(19) | H21C | 0.115(19) |